Electronic Supplementary Information (ESI):

Probing the elastic response of lipid bilayers and nanovesicles to leaflet tensions *via* volume per lipid

Miftakh F. Zamaletdinov[a], Markus S. Miettinen[a,b], and Reinhard Lipowsky[a]

[a] Max Planck Institute of Colloids and Interfaces, Science Park Golm, 14424 Potsdam, Germany
[b] University of Bergen, Department of Chemistry, 5007 Bergen, and Computational Biology Unit, Department of Informatics, 5008 Bergen, Norway

This Electronic Supplementary Information contains:

Supplementary Text:

Supplementary Figures:

Supplementary Tables:

The tables provide the numerical values for the parameters and data discussed in the main text.

S1 Radii of nanovesicles from molecular densities

S1.1 CHAIN protocol for vesicle radii

For a spherical nanovesicle, the density and stress profiles depend only on the radial coordinate r, and the midsurface between the two bilayer leaflets can be characterized by its radius $r = R_{\mathrm{mid}}$. In order to compute the two leaflet tensions, we need to decompose the stress profile of the bilayer into two parts, corresponding to the inner leaflet with $r < R_{\mathrm{mid}}$ and to the outer leaflet with $r > R_{\mathrm{mid}}$, see eqn (45) in the *Methods* section of the main text.

In the CHAIN protocol for nanovesicles, the radius R_{mid} is taken to be the r-value, at which the density profile $\rho_{\mathrm{C}}(r)$ of the hydrophobic C beads has an extremum, which is a maximum in the DPD approach used here. Furthermore, this protocol involves two additional computational steps. [1, 2] First, the radii $R_{i\mathrm{H}}$ and $R_{o\mathrm{H}}$ of the inner and outer headgroup layers are located at the two maxima of the density profile $\rho_{\mathrm{H}}(r)$ for the headgroup beads. Second, the midsurface radii R_{il} and R_{ol} of the inner and outer leaflets are computed in terms of the three radii R_{mid}, $R_{i\mathrm{H}}$, and $R_{o\mathrm{H}}$ according to

$$R_{il} \equiv \frac{1}{2}\left(R_{i\mathrm{H}} + R_{\mathrm{mid}}\right) . \tag{S1}$$

and

$$R_{ol} \equiv \frac{1}{2}\left(R_{\mathrm{mid}} + R_{o\mathrm{H}}\right) . \tag{S2}$$

as in eqns (34) and (35) of the main text, which determine the areas of the spherical midsurfaces.

The areas per lipid, a_{il} and a_{ol}, in the inner and outer leaflets are then computed by dividing the areas of the midsurfaces by the number of lipids assembled within these leaflets, which leads to [1, 2]

$$a_{il} = \frac{4\pi R_{il}^2}{N_{il}} \quad \text{and} \quad a_{ol} = \frac{4\pi R_{ol}^2}{N_{ol}} . \tag{S3}$$

When the CHAIN protocol is used to determine the areas per lipid for the smallest nanovesicle, assembled from $N_{il} + N_{ol} = 1500$, one obtains the data in Fig. S5. Inspection of this figure reveals that the reference state of the nanovesicle with tensionless leaflets is obtained for $N_{ol} = 1100$ and $N_{il} = 400$. For this reference state, the optimal areas per lipid, a_{il}^0 for the inner and a_{ol}^0 for the outer leaflet, are given by

$$a_{il}^0 = (1.682 \pm 0.002)\, d^2 \quad \text{and} \quad a_{ol}^0 = (1.096 \pm 0.001)\, d^2 , \tag{S4}$$

corresponding to the vertical dotted lines in Fig. S5. In fact, the area per lipid, a_{il}, in the inner leaflet is found to be always larger than the area per lipid, a_{ol}, in the outer leaflet, as shown in Fig. S5a for the whole range of N_{ol} values and by the blue data in Fig. 11 of the main text, which displays the optimal areas per lipid in the two leaflets for different vesicle sizes.

S1.2 Alternative protocol based on headgroup layers

A previous simulation study based on the Martini force field applied another protocol to obtain the areas per lipid, a_{il} and a_{ol}, in the two leaflets of a vesicle bilayer. [3] In this study, the radii of the two leaflets were identified with the radii of the two head group layers, which were defined by the location of the phosphate groups. In the coarse-grained molecular model used here, the head groups are described by the H beads, see Fig. 13 in the main text. Therefore, the procedure in Ref [3] implies the alternative definitions

$$R_{il} \equiv R_{i\mathrm{H}} \quad \text{and} \quad R_{ol} \equiv R_{o\mathrm{H}} \tag{S5}$$

for the radii of the inner and outer leaflets. Compared to eqns (S1) and (S2), the alternative definitions in eqn (S5) lead to a reduced value of the inner leaflet radius R_{il} and to an increased value of the outer leaflet radius R_{ol}.

Using the alternative definitions for the midsurfaces of the leaflets as given in eqn (S5), we again compute the areas per lipid in the two leaflets *via* eqn (S3). In order to obtain the leaflet tensions, we determine the location $r = r_{\rm mid}$ of the midsurfaces by the CHAIN protocol and decompose the stress profiles into their leaflet contributions corresponding to $r < R_{\rm mid}$ and $r > R_{\rm mid}$. The optimal lipid areas, a^0_{il} and a^0_{ol}, corresponding to the reference states with tensionless leaflets, are displayed by the red data symbols in Fig. S6; the numerical values of these data are in Table S13. Inspection of the red data in Fig. S6 reveals that the optimal area per lipid now increases with increasing mean curvature, where the mean curvatures of the inner and outer leaflets are taken to be negative and positive as in the main text. This functional dependence of the red data is opposite to the behavior of the blue data in Fig. 11 and Fig. S6. Thus, in contrast to the red data, the blue data for the optimal areas per lipid decrease with increasing mean curvature of the two leaflets, in agreement with the green data in Fig. 11 and Fig. S6 as obtained by the VORON protocol.

References

[1] R. Ghosh, V. Satarifard, A. Grafmüller, and R. Lipowsky. Spherical Nanovesicles Transform into a Multitude of Nonspherical Shapes. *Nano Lett.*, 19:7703–7711, 2019.

[2] A. Sreekumari and R. Lipowsky. Large stress asymmetries of lipid bilayers and nanovesicles generate lipid flip-flops and bilayer instabilities. *Soft Matter*, 18:6066–6078, 2022.

[3] H. J. Risselada and S. J. Marrink. Curvature effects on lipid packing and dynamics in liposomes revealed by coarse grained molecular dynamics simulations. *Phys. Chem. Chem. Phys.*, 11:2056–2067, 2009.

S2 Supplementary Figures

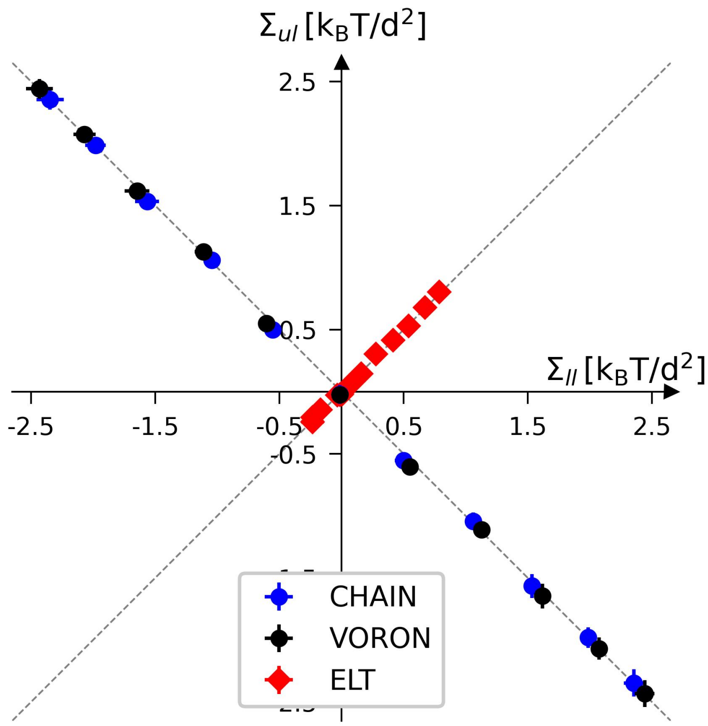

Figure S1: Leaflet tension space for planar bilayers that contain a total number of $N_{ll} + N_{ul} = 1682$ lipids. The two coordinates are the leaflet tensions Σ_{ll} and Σ_{ul} in the lower and upper leaflets. Negative and positive leaflet tensions describe compressed and stretched leaflets. The reference state with tensionless leaflets, corresponding to $\Sigma_{ll} = \Sigma_{ul} = 0$, is obtained for the symmetric bilayer with $N_{ll} = N_{ul} = 841$ lipids. The red data points describe elastic deformations with equal leaflet tensions (ELT), $\Sigma_{ll} = \Sigma_{ul}$, for which the midplane is equal to the plane of symmetry. The blue and black data represent bilayers with opposite leaflet tensions (OLT), $\Sigma_{ll} = -\Sigma_{ul}$. All OLT states can be obtained from the reference state by reshuffling lipids from one leaflet to the other and adjusting the base area of the simulation box to obtain tensionless bilayers. The blue data points are obtained from the CHAIN protocol, whereas the black data points are obtained from the VORON protocol. Adjacent blue and black data points are obtained for the same values of the lipid numbers N_{ll} and N_{ul} in the two leaflets. It then follows that the leaflet tensions $\Sigma_{ll} = -\Sigma_{ul}$ as obtained from the CHAIN protocol are smaller than those from the VORON protocol.

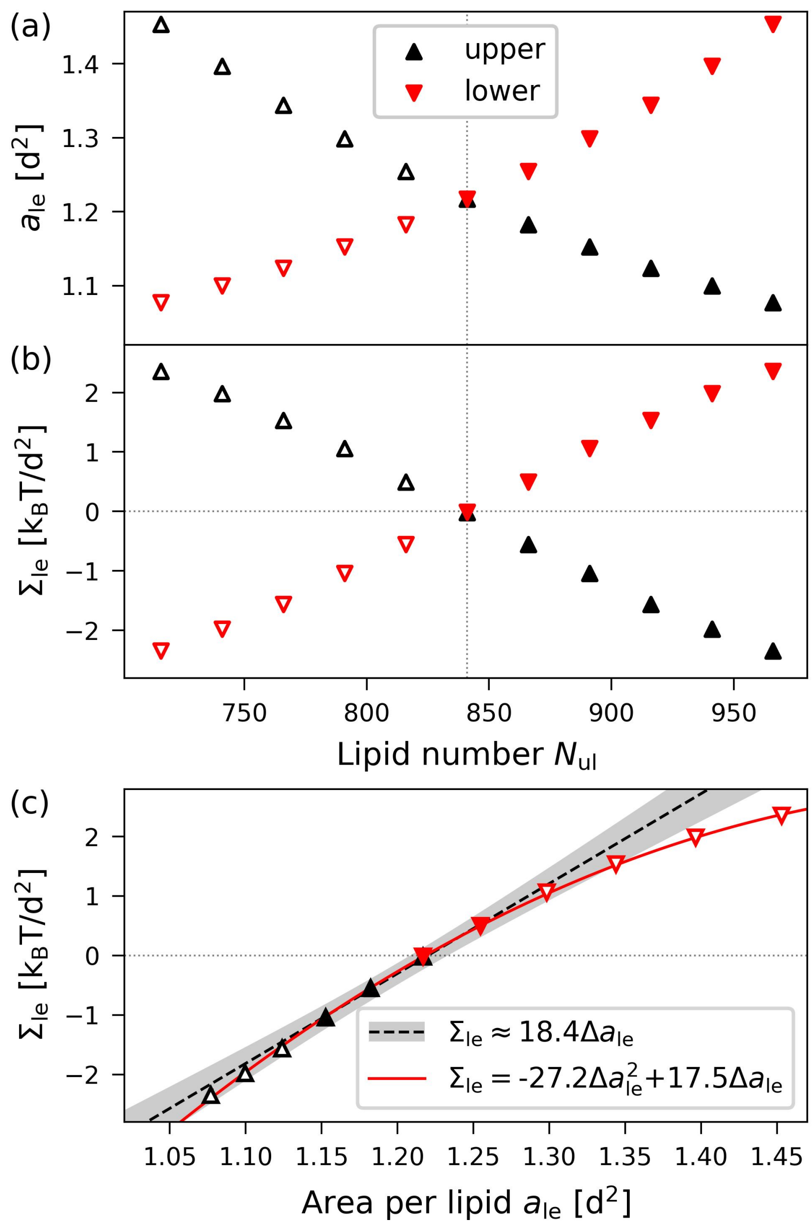

Figure S2: Elastic OLT deformations for planar bilayer with total lipid number $N_{ll}+N_{ul} = 1682$ as computed *via* the CHAIN protocol: (a) Areas per lipid and (b) Leaflet tensions as functions of the lipid number N_{ul} in the upper leaflet. Black up-triangles correspond to the upper leaflet and red down-triangles to the lower one. In (a) and (b), filled data points are the results of simulations, hollow data points are obtained by interchanging the lipid numbers and leaflet tensions between the two leaflets according to $N'_{ll} = N_{ul}$, $N'_{ul} = N_{ll}$, $\Sigma'_{ll} = \Sigma_{ul}$, and $\Sigma'_{ul} = \Sigma_{ll}$; and (c) Leaflet tensions versus projected area per lipid, a_{le}. The red line represents the least squares fit to all data points using the second-order expression in eqn (14) of the main text. The dashed black line provides the best fit to the filled data symbols in (c), which represent those data that fulfill the linearity condition $|\Delta a_{\text{le}}| < K_{\text{OLT}}/10K'$. The gray shaded band indicates the 95% prediction band for the linear fit. The numerical values of the data are displayed in Table S6. The corresponding data from the VORON protocol are displayed in Fig. 5 in the main text.

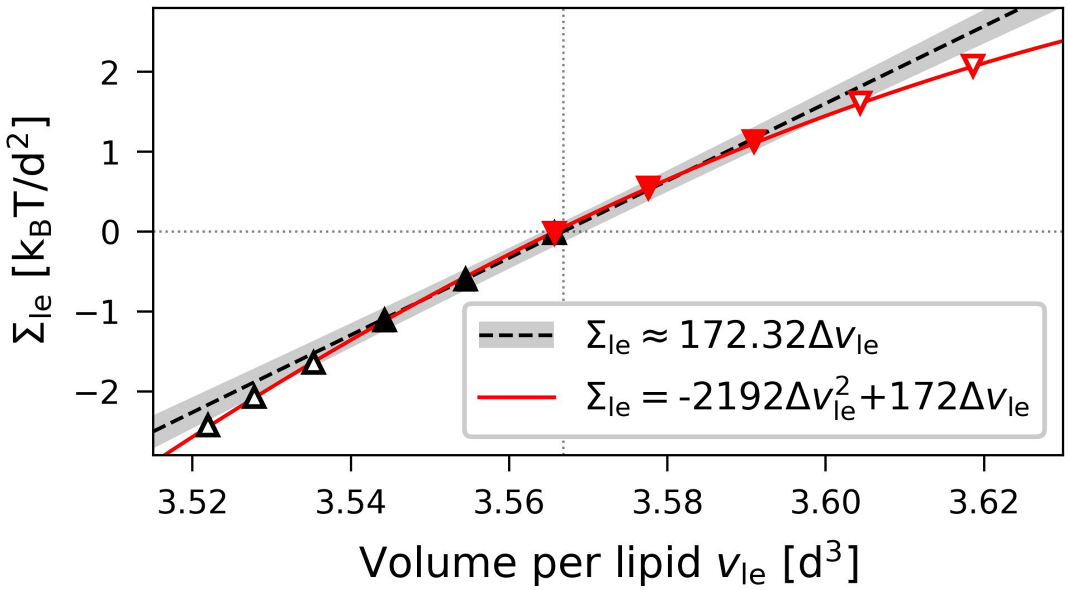

Figure S3: OLT deformations of planar bilayer assembled from $N_{ll} + N_{ul} = 1682$ lipids. Leaflet tensions Σ_{ul} and Σ_{ll} as functions of the volume per lipid, $v_{\rm le}$. The data shown here are identical with those in Fig. 7 of the main text, with the midplanes of the asymmetric OLT states computed by the VORON protocol, but including a least squares fit (red line) of all data to the second-order expression in eqn (20) of the main text. The dotted vertical line is located at the optimal lipid volume $v = v^0 = 3.566\, d^3$. Filled data symbols represent those v-values for which the linearity condition $|\Delta v| < B_{\rm OLT}/(10B')$ is fulfilled. The dashed black line represents the best linear fit to the filled data symbols, the grey shaded band represents the 95% prediction band. The numerical values of the data are in Table S3.

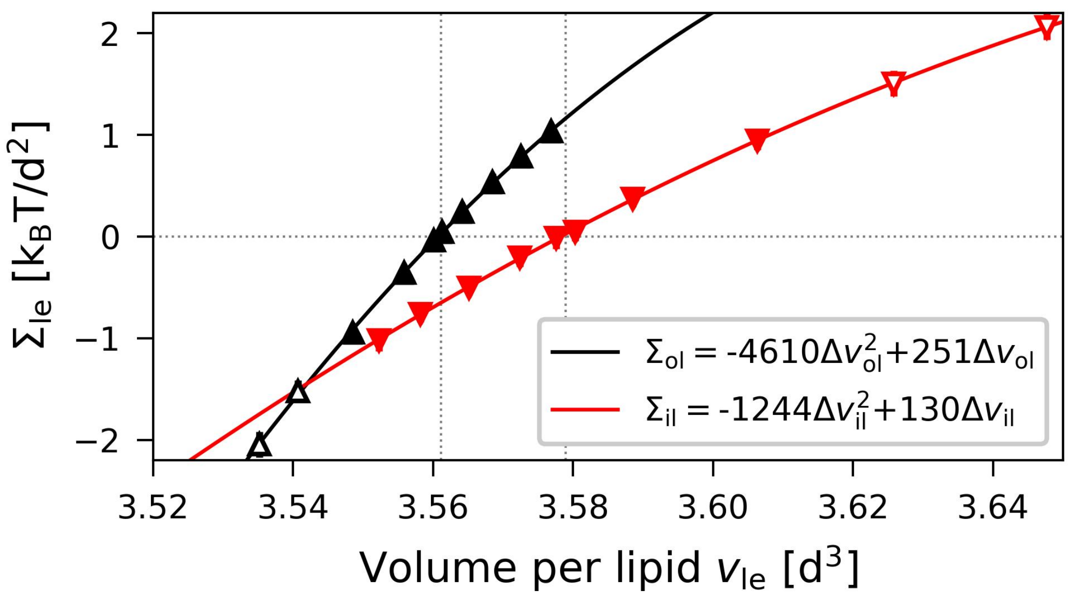

Figure S4: Elastic OLT deformations of the smallest nanovesicles with a total number of $N_{il} + N_{ol} = 1500$ lipids: Leaflet tensions $\Sigma_{\mathrm{le}} = \Sigma_{ol}$ and Σ_{il} of the outer (black data, up-pointing triangles) and inner leaflets (red data, down-pointing triangles) versus volumes per lipid, $v_{\mathrm{le}} = v_{il}$ and $v_{\mathrm{le}} = v_{ol}$, in the two leaflets of the tensionless bilayers. The data shown here are identical with those in Fig. 8 of the main text, with the midplanes of the asymmetric OLT states computed by the VORON protocol. The black and red lines represent the least squares fits of the data to the second-order expression in eqn (20) of the main text, where the subscript 'le' now stands for *ol* and *il*, corresponding to the outer and inner leaflets. The two dotted vertical lines are located at the optimal lipid volumes $v = v^0_{ol} \simeq 3.56\, d^3$ and $v = v^0_{il} \simeq 3.58\, d^3$ of the outer and inner leaflets. The numerical values of the data are in Table S7.

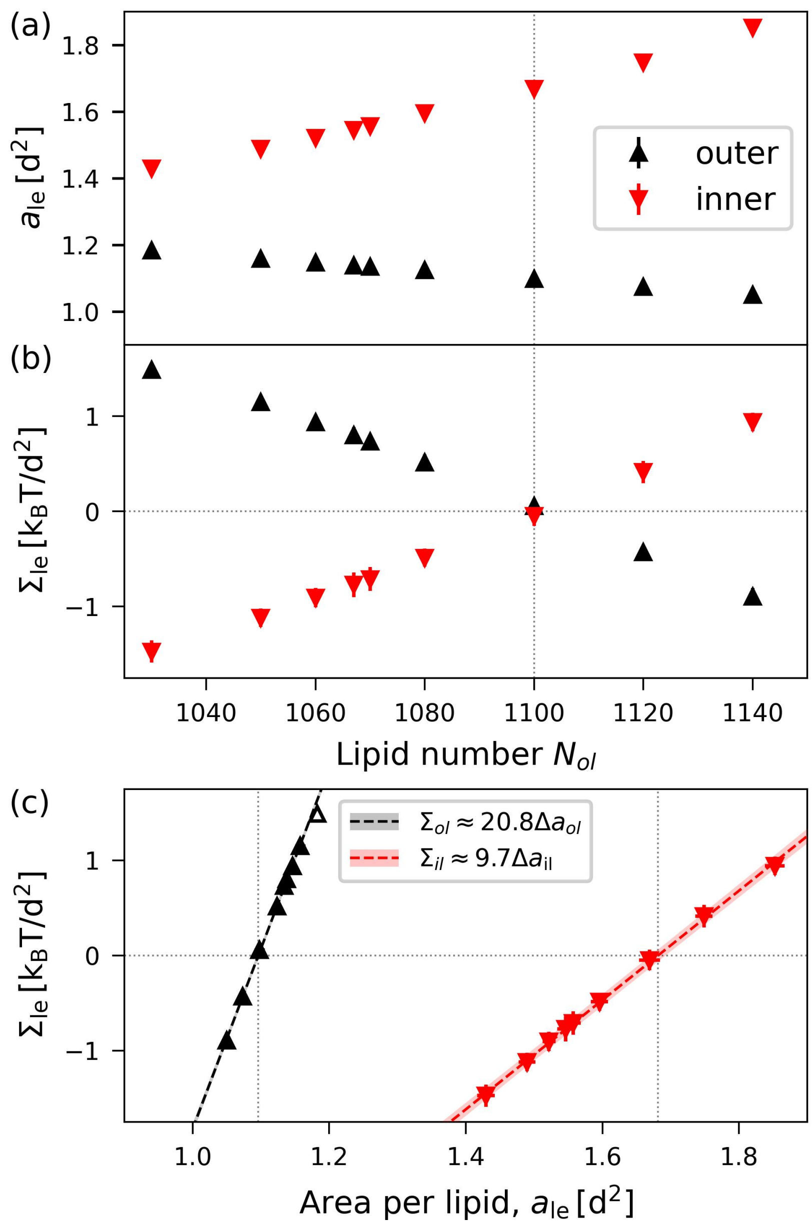

Figure S5: Elastic OLT deformations of the smallest nanovesicles with a total number of $N_{il} + N_{ol} = 1500$ lipids in both leaflets as computed by the CHAIN protocol (Section S1.1): (a,b) Areas per lipid, a_{il} and a_{ol}, as well as leaflet tensions Σ_{il} and Σ_{ol} of the inner and outer leaflets as functions of the lipid number N_{ol} in the outer leaflet. The midsurfaces of the vesicle bilayers are determined via the CHAIN protocol, and the areas per lipid are computed as described in ... The reference state with tensionless leaflets corresponds to the vertical dotted lines at $N_{ol} = N_{ol}^0 = 1100$; and (c) Leaflet tensions Σ_{il} and Σ_{ol} as functions of the lipid areas. The data for the inner leaflet are in red, those for the outer leaflet in black. The vertical dotted lines in (c) represent the optimal areas per lipid as given by $a_{ol}^0 = 1.096\, d^2$ and $a_{il}^0 = 1.682\, d^2$ for the outer and inner leaflet, respectively. The numerical values of the data are displayed in Table S10. The corresponding data as obtained from the VORON protocol are displayed in Fig. 10 of the main text.

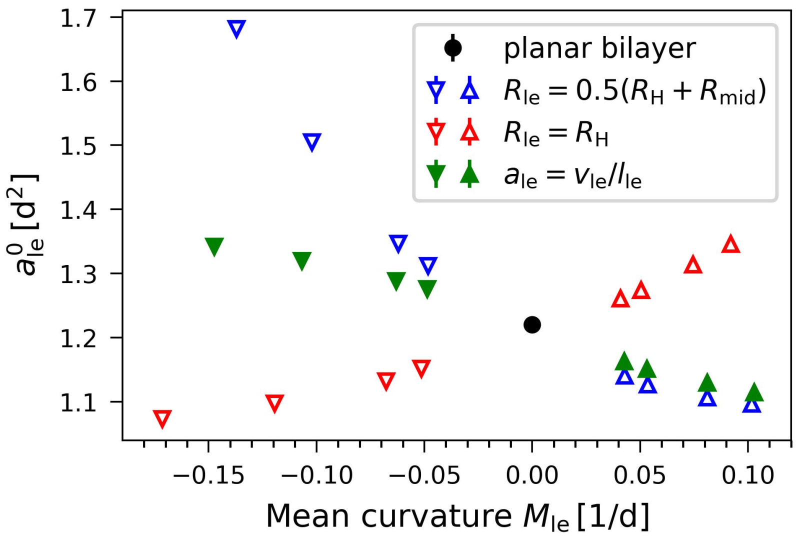

Figure S6: Optimal areas per lipid, $a^0_{\mathrm{le}} = a^0_{il}$ and a^0_{ol}, for the inner and outer leaflets versus the mean curvature $M_{\mathrm{le}} = M_{il}$ and M_{ol} of the two leaflets, as determined by three different computational methods provided by the VORON protocol (green data symbols), CHAIN protocol (blue data symbols), and the procedure described in Section S1.2 [3] based on the headgroup layers. The green and blue data, which are identical with those in Fig. 11 of the main text, predict that the area per lipid, a^0_{le}, decreases monotonically with increasing mean curvature and that, for each nanovesicle, the optimal area per lipid, a^0_{il}, in the inner leaflet is always larger than the optimal area per lipid, a^0_{ol}, in the outer leaflet. This behavior is consistent with the intuitive view that lipids with two hydrocarbon chains prefer to reside in the more weakly curved surface, as provided by the outer leaflet, rather than in the more strongly curved inner leaflet. In contrast, the red data predict the opposite behavior, that is, that the areas per lipid in the outer leaflets are always larger than the areas per lipid in the inner leaflets. The numerical values of the green data are in Table S8, those of the blue and red data in Table S13.

,

S3 Supplementary tables for planar bilayers

Table S1: Area compressibility modulus $K_{\rm ELT}$ and optimal area per lipid, a^0, as obtained for ELT deformations of planar and symmetric bilayers, for three different values of the total lipid number $N_{\rm lip} = N_{ll} + N_{ul}$.

$N_{\rm lip}$	$K_{\rm ELT}$ $[k_{\rm B}T/d^2]$	a^0 $[d^2]$
1200	13.47 ± 0.28	1.2193 ± 0.0010
1682	13.38 ± 0.14	1.2183 ± 0.0004
2000	13.17 ± 0.03	1.21753 ± 0.00008

Table S2: ELT deformations of planar and symmetric bilayers with total lipid numbers $N_{\rm lip} = N_{ll} + N_{ul} = 2000, 1682$ and 1200 as determined by the VORON protocol: Projected area per lipid, $a_{\rm le} = a_{ll} = a_{ul}$; volume per lipid, $v_{\rm le} = v_{ll} = v_{ul}$; and leaflet tensions $\Sigma_{\rm le} = \Sigma_{ll} = \Sigma_{ul}$. For $N_{ll} = N_{ul} = 841$, the dependence of $\Sigma_{\rm le}$ on $a_{\rm le}$ is plotted in Fig. 4c the dependence of $\Sigma_{\rm le}$ on $v_{\rm le}$ in Fig. 6.

(a) $N_{\rm lip} = 2000$

$a_{\rm le}$ $[d^2]$	$v_{\rm le}$ $[d^3]$	$\Sigma_{\rm le}$ $[k_{\rm B}T/d^2]$
1.289	3.5833 ± 0.0007	0.77 ± 0.03
1.278	3.5806 ± 0.0006	0.65 ± 0.03
1.257	3.5750 ± 0.0006	0.42 ± 0.03
1.246	3.5722 ± 0.0006	0.31 ± 0.04
1.236	3.5696 ± 0.0006	0.19 ± 0.03
1.225	3.5672 ± 0.0007	0.08 ± 0.04
1.216	3.5658 ± 0.0007	-0.01 ± 0.04

(b) $N_{\rm lip} = 1682$

$a_{\rm le}$ $[d^2]$	$v_{\rm le}$ $[d^3]$	$\Sigma_{\rm le}$ $[k_{\rm B}T/d^2]$
1.291	3.5838 ± 0.0008	0.80 ± 0.03
1.279	3.5809 ± 0.0007	0.67 ± 0.04
1.268	3.5780 ± 0.0008	0.53 ± 0.05
1.256	3.5747 ± 0.0008	0.42 ± 0.04
1.244	3.5717 ± 0.0007	0.29 ± 0.05
1.233	3.5693 ± 0.0006	0.15 ± 0.04
1.222	3.5666 ± 0.0007	0.06 ± 0.04
1.218	3.5657 ± 0.0007	-0.01 ± 0.04
1.215	3.5651 ± 0.0008	-0.03 ± 0.06
1.202	3.5629 ± 0.0009	-0.16 ± 0.04
1.191	3.5613 ± 0.0008	-0.22 ± 0.06
1.180	3.5611 ± 0.0011	-0.24 ± 0.06

(c) $N_{\rm lip} = 1200$

$a_{\rm le}$ $[d^2]$	$v_{\rm le}$ $[d^3]$	$\Sigma_{\rm le}$ $[k_{\rm B}T/d^2]$
1.302	3.5865 ± 0.0007	0.90 ± 0.05
1.288	3.5831 ± 0.0009	0.77 ± 0.05
1.274	3.5794 ± 0.0008	0.60 ± 0.04
1.260	3.5758 ± 0.0008	0.47 ± 0.04
1.247	3.5720 ± 0.0007	0.30 ± 0.05
1.233	3.5692 ± 0.0010	0.17 ± 0.05
1.223	3.5666 ± 0.0010	0.03 ± 0.04

Table S3: OLT deformations of planar bilayers with three different values of the total lipid number $N_{\text{lip}} = N_{ul} + N_{ll}$: Lipid number N_{ul} and volume per lipid, v_{ul}, in the upper leaflet; volume per lipid, v_{ll}, in the lower leaflet; and leaflet tensions Σ_{ul} and Σ_{ll} in the upper and lower leaflets. The leaflet tensions were computed using the VORON protocol for the location z_{mid} of the midplane as in eqns (3) and (4) of the main text. The dependence of the two leaflet tensions on the area per lipid is plotted in Fig. 5c for $N_{\text{lip}} = 1682$, the dependence of the leaflet tensions on the volume per lipid in Fig. 7 and Fig. S3.

(a) $N_{\text{lip}} = 2000$

N_{ul}	a_{ul} $[d^2]$	a_{ll} $[d^2]$	v_{ul} $[d^3]$	v_{ll} $[d^3]$	Σ_{ul} $[k_{\text{B}}T/d^2]$	Σ_{ll} $[k_{\text{B}}T/d^2]$
1000	1.216	1.216	3.5656±0.0007	3.5654±0.0008	-0.04 ± 0.05	-0.02 ± 0.05
1030	1.184	1.257	3.5547±0.0006	3.5783±0.0007	-0.56 ± 0.05	0.57 ± 0.05
1060	1.150	1.296	3.5439±0.0007	3.5909±0.0009	-1.14 ± 0.09	1.10 ± 0.05
1090	1.119	1.340	3.5343±0.0007	3.6039±0.0007	-1.64 ± 0.10	1.54 ± 0.06
1120	1.101	1.402	3.5282±0.0007	3.6188±0.0007	-2.05 ± 0.12	2.09 ± 0.07

(b) $N_{\text{lip}} = 1682$

N_{ul}	a_{ul} $[d^2]$	a_{ll} $[d^2]$	v_{ul} $[d^3]$	v_{ll} $[d^3]$	Σ_{ul} $[k_{\text{B}}T/d^2]$	Σ_{ll} $[k_{\text{B}}T/d^2]$
841	1.217	1.217	3.5657±0.0007	3.5657±0.0008	-0.02 ± 0.07	-0.01 ± 0.06
866	1.182	1.255	3.5545±0.0009	3.5776±0.0006	-0.60 ± 0.05	0.55 ± 0.06
891	1.153	1.299	3.5443±0.0007	3.5910±0.0009	-1.11 ± 0.07	1.13 ± 0.05
916	1.124	1.344	3.5353±0.0007	3.6044±0.0007	-1.65 ± 0.10	1.62 ± 0.04
941	1.100	1.397	3.5278±0.0006	3.6187±0.0009	-2.07 ± 0.09	2.07 ± 0.05
966	1.077	1.454	3.5219±0.0008	3.6329±0.0006	-2.43 ± 0.11	2.44 ± 0.08

(c) $N_{\text{lip}} = 1200$

N_{ul}	a_{ul} $[d^2]$	a_{ll} $[d^2]$	v_{ul} $[d^3]$	v_{ll} $[d^3]$	Σ_{ul} $[k_{\text{B}}T/d^2]$	Σ_{ll} $[k_{\text{B}}T/d^2]$
600	1.220	1.220	3.5656±0.0009	3.5659±0.0009	-0.00 ± 0.06	0.00 ± 0.07
618	1.186	1.259	3.5547±0.0007	3.5784±0.0009	-0.59 ± 0.06	0.60 ± 0.06
636	1.153	1.300	3.5442±0.0011	3.5911±0.0009	-1.17 ± 0.08	1.15 ± 0.06
654	1.127	1.350	3.5352±0.0009	3.6051±0.0009	-1.70 ± 0.09	1.70 ± 0.07
671	1.086	1.377	3.5261±0.0009	3.6160±0.0012	-2.22 ± 0.16	1.93 ± 0.07

Table S4: Area compressibility modulus K_{OLT} and optimal area per lipid, a^0, as obtained for OLT deformations of planar bilayers and computed by the VORON protocol, for three different values of the total lipid number $N_{\text{lip}} = N_{ll} + N_{ul}$.

N_{lip}	K_{OLT} $[k_{\text{B}}T/d^2]$	a^0 $[d^2]$
1200	20.1 ± 0.7	1.2246 ± 0.0021
1682	19.9 ± 0.5	1.2197 ± 0.0011
2000	19.5 ± 0.6	1.2198 ± 0.0013

Table S5: Lateral volume compressibilities B_{ELT} and B_{OLT} for ELT and OLT deformations of planar bilayers as well as optimal volumes per lipid, v^0, as computed for three different values of the total lipid number $N_{\text{lip}} = N_{ll} + N_{ul}$ by the VORON protocol.

(a) ELT deformations

N_{lip}	B_{ELT} $[k_{\text{B}}T/d^2]$	v^0 $[d^3]$
1200	154 ± 3	3.56541 ± 0.00028
1682	156 ± 3	3.56553 ± 0.00020
2000	156 ± 4	3.56548 ± 0.00022

(b) OLT deformations

N_{lip}	B_{OLT} $[k_{\text{B}}T/d^2]$	v^0 $[d^3]$
1200	184 ± 4	3.5664 ± 0.0003
1682	172 ± 4	3.5668 ± 0.0003
2000	170 ± 4	3.5669 ± 0.0004

Table S6: OLT deformations of planar bilayers for total lipid numbers $N_{\rm lip} = N_{ll} + N_{ul} = 2000, 1682$ and 1200: Lipid number N_{ul} and area per lipid, a_{ul}, in the upper leaflet; area per lipid, a_{ll}, in the lower leaflet; and leaflet tensions Σ_{ul} and Σ_{ll} in the upper and lower leaflet. The leaflet tensions were computed using the CHAIN protocol, that is, by identifying the location $z_{\rm mid}$ of the midplane with the maximum of the C bead density. The lipid number N_{ll} in the lower leaflet is equal to $N_{\rm lip} - N_{ul}$. For $N_{\rm lip} = 1682$, the areas per lipid are plotted in Fig. S2a, the leaflet tensions in Fig. S2b as functions of the lipid number N_{ul} in the upper leaflet.

(a) $N_{\rm lip} = 2000$

N_{ul}	$a_{ul}\,[d^2]$	$a_{ll}\,[d^2]$	$\Sigma_{ul}\,[k_{\rm B}T/d^2]$	$\Sigma_{ll}\,[k_{\rm B}T/d^2]$
1000	1.216	1.216	-0.05 ± 0.06	-0.01 ± 0.06
1030	1.184	1.257	-0.53 ± 0.06	0.53 ± 0.06
1060	1.150	1.296	-1.08 ± 0.09	1.04 ± 0.06
1090	1.119	1.340	-1.57 ± 0.09	1.47 ± 0.06
1120	1.101	1.402	-1.95 ± 0.11	1.99 ± 0.08

(b) $N_{\rm lip} = 1682$

$N_{\rm ul}$	$a_{\rm ul}\,[d^2]$	$a_{\rm ll}\,[d^2]$	$\Sigma_{\rm ul}\,[k_{\rm B}T/d^2]$	$\Sigma_{\rm ll}\,[k_{\rm B}T/d^2]$
841	1.217	1.217	-0.02 ± 0.08	-0.01 ± 0.07
866	1.182	1.255	-0.55 ± 0.05	0.50 ± 0.07
891	1.153	1.299	-1.04 ± 0.07	1.06 ± 0.06
916	1.124	1.344	-1.56 ± 0.10	1.53 ± 0.05
941	1.100	1.397	-1.98 ± 0.08	1.98 ± 0.05
966	1.077	1.454	-2.35 ± 0.11	2.35 ± 0.08

(c) $N_{\rm lip} = 1200$

$N_{\rm ul}$	$a_{\rm ul}\,[d^2]$	$a_{\rm ll}\,[d^2]$	$\Sigma_{\rm ul}\,[k_{\rm B}T/d^2]$	$\Sigma_{\rm ll}\,[k_{\rm B}T/d^2]$
600	1.220	1.220	0.00 ± 0.08	0.00 ± 0.09
618	1.186	1.259	-0.52 ± 0.06	0.54 ± 0.08
636	1.153	1.300	-1.06 ± 0.08	1.05 ± 0.08
654	1.127	1.350	-1.56 ± 0.08	1.56 ± 0.07
671	1.086	1.377	-2.15 ± 0.15	1.85 ± 0.07

S4 Supplementary tables for nanovesicles

Table S7: OLT deformations of vesicle bilayers with four different lipid numbers $N_{\text{lip}} = N_{il} + N_{ol}$ as obtained by the VORON protocol: The columns display the lipid number N_{ol} in the outer leaflet for fixed N_{lip}; the volumes per lipid, v_{il} and v_{ol} in the inner and outer leaflets; the areas per lipid, a_{il} and a_{ol}, computed via eqns (33) and (34) in the main text; as well as the inner and outer leaflet tensions Σ_{il} and Σ_{ol}, which were obtained by computing the midsurface radii R_{mid} of the vesicle bilayer in terms of the volumes, see eqns (29) and (30) in the main text.

(a) $N_{\text{lip}} = 10100$

N_{ol}	v_{il} $[d^3]$	v_{ol} $[d^3]$	a_{il} $[d^2]$	a_{ol} $[d^2]$	Σ_{il} $[k_BT/d^2]$	Σ_{ol} $[k_BT/d^2]$
5700	3.5527 ± 0.0005	3.5782 ± 0.0004	1.21032 ± 0.00004	1.219436 ± 0.000015	-0.81 ± 0.05	0.84 ± 0.04
5800	3.5608 ± 0.0003	3.5709 ± 0.0004	1.23481 ± 0.00004	1.195486 ± 0.000017	-0.49 ± 0.05	0.52 ± 0.04
5900	3.5695 ± 0.0004	3.5640 ± 0.0004	1.26179 ± 0.00004	1.173175 ± 0.000013	-0.16 ± 0.05	0.18 ± 0.06
5954	3.5746 ± 0.0004	3.5603 ± 0.0003	1.27622 ± 0.00003	1.161036 ± 0.000014	0.02 ± 0.06	0.00 ± 0.06
6000	3.5788 ± 0.0003	3.5572 ± 0.0005	1.28899 ± 0.00004	1.150954 ± 0.000012	0.18 ± 0.06	-0.18 ± 0.07
6100	3.5885 ± 0.0004	3.5508 ± 0.0004	1.31770 ± 0.00005	1.129557 ± 0.000017	0.48 ± 0.06	-0.48 ± 0.08
6300	3.6100 ± 0.0004	3.5392 ± 0.0005	1.38839 ± 0.00005	1.093445 ± 0.000010	1.11 ± 0.10	-1.11 ± 0.13

(b) $N_{\text{lip}} = 6312$

N_{ol}	v_{il} $[d^3]$	v_{ol} $[d^3]$	a_{il} $[d^2]$	a_{ol} $[d^2]$	Σ_{il} $[k_BT/d^2]$	Σ_{ol} $[k_BT/d^2]$
3641	3.5456 ± 0.0004	3.5836 ± 0.0005	1.19270 ± 0.00005	1.228054 ± 0.000028	-1.18 ± 0.07	1.18 ± 0.04
3741	3.5581 ± 0.0004	3.5724 ± 0.0004	1.23410 ± 0.00007	1.19096 ± 0.00003	-0.66 ± 0.05	0.67 ± 0.06
3841	3.5725 ± 0.0006	3.5616 ± 0.0005	1.27944 ± 0.00006	1.15613 ± 0.00003	-0.10 ± 0.05	0.12 ± 0.07
3858	3.5753 ± 0.0004	3.5597 ± 0.0004	1.28742 ± 0.00005	1.150342 ± 0.000024	0.01 ± 0.05	0.01 ± 0.06
3881	3.5787 ± 0.0004	3.5573 ± 0.0004	1.29846 ± 0.00005	1.142612 ± 0.000025	0.12 ± 0.08	-0.11 ± 0.08
3941	3.5886 ± 0.0004	3.5514 ± 0.0004	1.33040 ± 0.00005	1.123999 ± 0.000026	0.49 ± 0.07	-0.47 ± 0.09
4041	3.6065 ± 0.0006	3.5420 ± 0.0006	1.38595 ± 0.00008	1.093530 ± 0.000028	1.01 ± 0.10	-1.02 ± 0.15

(c) $N_{\text{lip}} = 2525$

N_{ol}	v_{il} $[d^3]$	v_{ol} $[d^3]$	a_{il} $[d^2]$	a_{ol} $[d^2]$	Σ_{il} $[k_BT/d^2]$	Σ_{ol} $[k_BT/d^2]$
1575	3.5375 ± 0.0006	3.5894 ± 0.0006	1.17141 ± 0.00012	1.22230 ± 0.00004	-1.61 ± 0.09	1.62 ± 0.05
1625	3.5528 ± 0.0006	3.5760 ± 0.0005	1.23760 ± 0.00012	1.18107 ± 0.00006	-0.97 ± 0.07	0.95 ± 0.05
1650	3.5618 ± 0.0008	3.5696 ± 0.0006	1.26833 ± 0.00015	1.15938 ± 0.00005	-0.59 ± 0.05	0.60 ± 0.07
1675	3.5715 ± 0.0005	3.5631 ± 0.0007	1.30090 ± 0.00016	1.13833 ± 0.00005	-0.21 ± 0.08	0.22 ± 0.08
1685	3.5756 ± 0.0006	3.5604 ± 0.0006	1.31396 ± 0.00017	1.12989 ± 0.00005	-0.05 ± 0.07	0.04 ± 0.08
1687	3.5767 ± 0.0006	3.5603 ± 0.0006	1.31639 ± 0.00017	1.12817 ± 0.00005	-0.05 ± 0.06	0.04 ± 0.08
1695	3.5800 ± 0.0007	3.5579 ± 0.0005	1.32732 ± 0.00011	1.12156 ± 0.00005	0.09 ± 0.07	-0.11 ± 0.09
1699	3.5817 ± 0.0005	3.5570 ± 0.0006	1.33230 ± 0.00017	1.11809 ± 0.00005	0.17 ± 0.07	-0.17 ± 0.09
1725	3.5937 ± 0.0008	3.5508 ± 0.0006	1.37399 ± 0.00015	1.09875 ± 0.00005	0.61 ± 0.10	-0.61 ± 0.10
1775	3.6201 ± 0.0007	3.5396 ± 0.0007	1.46171 ± 0.00015	1.06303 ± 0.00004	1.45 ± 0.10	-1.43 ± 0.12
1825	3.6483 ± 0.0008	3.5309 ± 0.0006	1.56825 ± 0.00019	1.03119 ± 0.00005	2.11 ± 0.13	-2.10 ± 0.18

(d) $N_{\text{lip}} = 1500$; leaflet tensions are plotted in Fig. 8 versus volume per lipid.

N_{ol}	v_{il} $[d^3]$	v_{ol} $[d^3]$	a_{il} $[d^2]$	a_{ol} $[d^2]$	Σ_{il} $[k_BT/d^2]$	Σ_{ol} $[k_BT/d^2]$
1030	3.5523 ± 0.0009	3.5768 ± 0.0006	1.24550 ± 0.00022	1.16589 ± 0.00008	-1.02 ± 0.11	1.03 ± 0.05
1040	3.5582 ± 0.0011	3.5726 ± 0.0007	1.26934 ± 0.00021	1.15154 ± 0.00008	-0.76 ± 0.08	0.79 ± 0.08
1050	3.5652 ± 0.0010	3.5685 ± 0.0007	1.29439 ± 0.00025	1.13757 ± 0.00009	-0.50 ± 0.08	0.53 ± 0.09
1060	3.5724 ± 0.0008	3.5642 ± 0.0008	1.32041 ± 0.00021	1.12378 ± 0.00008	-0.21 ± 0.09	0.24 ± 0.07
1067	3.5776 ± 0.0009	3.5613 ± 0.0006	1.33929 ± 0.00024	1.11426 ± 0.00007	-0.01 ± 0.11	0.04 ± 0.06
1070	3.5803 ± 0.0010	3.5601 ± 0.0006	1.34772 ± 0.00024	1.11030 ± 0.00006	0.05 ± 0.10	-0.04 ± 0.08
1080	3.5885 ± 0.0008	3.5559 ± 0.0008	1.3762 ± 0.0003	1.09700 ± 0.00008	0.37 ± 0.09	-0.36 ± 0.06
1100	3.6063 ± 0.0009	3.5485 ± 0.0007	1.43604 ± 0.00026	1.07086 ± 0.00008	0.94 ± 0.09	-0.95 ± 0.08
1120	3.6258 ± 0.0010	3.5407 ± 0.0007	1.4992 ± 0.0003	1.04486 ± 0.00009	1.51 ± 0.13	-1.52 ± 0.11
1140	3.6477 ± 0.0013	3.5352 ± 0.0007	1.5884 ± 0.0003	1.02414 ± 0.00007	2.06 ± 0.13	-2.05 ± 0.12

Table S8: Lateral volume compressibilities and optimal volumes per lipid for inner and outer leaflets of nanovesicles with four different total lipid numbers $N_{\text{lip}} = N_{il} + N_{ol}$ as obtained from the VORON protocol. The rows display the mean curvatures M_{il} and M_{ol}; the lateral volume compressibility moduli B_{il} and B_{ol} for OLT deformations; as well as the optimal areas per lipid, v^0_{il} and v^0_{ol} of the inner and outer leaflets, respectively. The optimal volumes per lipid and the lateral volume compressibility moduli are plotted in Fig. 9 of the main text.

N_{lip}	10100	6312	2525	1500
M_{il} $[1/d]$	-0.049	-0.063	-0.107	-0.147
B_{il} $[k_{\text{B}}T/d^2]$	131 ± 3	135 ± 2	133 ± 4	130 ± 3
v^0_{il} $[d^3]$	3.57435 ± 0.00031	3.57538 ± 0.00015	3.5785 ± 0.0008	3.5790 ± 0.0004
M_{ol} $[1/d]$	0.043	0.053	0.081	0.103
B_{ol} $[k_{\text{B}}T/d^2]$	178 ± 3	198 ± 4	218 ± 7	248 ± 8
v^0_{ol} $[d^3]$	3.56073 ± 0.00019	3.5598 ± 0.00021	3.56005 ± 0.00028	3.56116 ± 0.00027

Table S9: Radii of vesicle bilayers with total lipid numbers $N_{\mathrm{lip}} = N_{il} + N_{ol} = 10100$, 6312, 2525, and 1500 as obtained form the VORON protocol *via* eqns (29) to (31) in the main text. The columns display the lipid number N_{ol} in the outer leaflet; the midsurface radius R_{mid} of the bilayer; and the radii $R_{i\mathrm{H}}$ and $R_{o\mathrm{H}}$ of the inner and outer head group layers.

(a) $N_{\mathrm{lip}} = 10100$

N_{ol}	R_{mid} [d]	$R_{i\mathrm{H}}$ [d]	$R_{o\mathrm{H}}$ [d]
5700	22.03622 ± 0.00020	19.1009 ± 0.0005	24.97052 ± 0.00023
5800	21.9806 ± 0.0003	19.0969 ± 0.0005	24.96757 ± 0.00017
5900	21.93406 ± 0.00023	19.1051 ± 0.0005	24.97200 ± 0.00021
5954	21.90431 ± 0.00018	19.1034 ± 0.0004	24.97084 ± 0.00020
6000	21.87998 ± 0.00023	19.1036 ± 0.0005	24.97060 ± 0.00024
6100	21.82673 ± 0.00029	19.1034 ± 0.0005	24.97024 ± 0.00022
6300	21.77635 ± 0.00025	19.1762 ± 0.0005	25.01307 ± 0.00022

(b) $N_{\mathrm{lip}} = 6312$

N_{ol}	R_{mid} [d]	$R_{i\mathrm{H}}$ [d]	$R_{o\mathrm{H}}$ [d]
3641	17.3853 ± 0.0003	14.4125 ± 0.0005	20.30341 ± 0.00026
3741	17.3097 ± 0.0004	14.4265 ± 0.0006	20.30931 ± 0.00026
3841	17.2370 ± 0.0003	14.4448 ± 0.0006	20.3176 ± 0.0003
3858	17.22422 ± 0.0003	14.4471 ± 0.0004	20.31873 ± 0.00024
3881	17.20706 ± 0.00027	14.4509 ± 0.0004	20.32036 ± 0.00026
3941	17.1731 ± 0.0003	14.4757 ± 0.0004	20.33268 ± 0.00028
4041	17.1095 ± 0.0004	14.5073 ± 0.0007	20.3485 ± 0.0004

(c) $N_{\mathrm{lip}} = 2525$

N_{ol}	R_{mid} [d]	$R_{i\mathrm{H}}$ [d]	$R_{o\mathrm{H}}$ [d]
1575	10.8799 ± 0.0003	7.8601 ± 0.0008	13.81649 ± 0.00028
1625	10.8135 ± 0.0004	7.9428 ± 0.0007	13.8413 ± 0.0003
1650	10.7667 ± 0.0005	7.9584 ± 0.0008	13.8455 ± 0.00028
1675	10.7197 ± 0.0005	7.9743 ± 0.0008	13.8498 ± 0.0003
1685	10.6995 ± 0.0004	7.9782 ± 0.0009	13.8506 ± 0.0003
1687	10.6950 ± 0.0005	7.9779 ± 0.0008	13.85079 ± 0.00027
1695	10.6793 ± 0.0004	7.9822 ± 0.0006	13.85159 ± 0.0003
1699	10.6700 ± 0.0005	7.9817 ± 0.0008	13.85136 ± 0.0003
1725	10.6298 ± 0.0005	8.0143 ± 0.0007	13.86151 ± 0.00028
1775	10.5511 ± 0.0004	8.0745 ± 0.0007	13.8808 ± 0.0004
1825	10.4856 ± 0.0005	8.1592 ± 0.0008	13.9097 ± 0.0004

(d) $N_{\mathrm{lip}} = 1500$

N_{ol}	R_{mid} [d]	$R_{i\mathrm{H}}$ [d]	$R_{o\mathrm{H}}$ [d]
1030	8.2014 ± 0.0005	5.3493 ± 0.0010	11.2693 ± 0.0003
1040	8.1699 ± 0.0006	5.3667 ± 0.0008	11.2723 ± 0.0003
1050	8.1388 ± 0.0006	5.3845 ± 0.0009	11.2758 ± 0.0004
1060	8.1072 ± 0.0005	5.4017 ± 0.0008	11.2788 ± 0.0005
1067	8.0849 ± 0.0005	5.4137 ± 0.0009	11.2810 ± 0.0003
1070	8.0758 ± 0.0004	5.4192 ± 0.0011	11.2822 ± 0.0003
1080	8.0439 ± 0.0007	5.4363 ± 0.0010	11.2853 ± 0.0004
1100	7.9776 ± 0.0005	5.4663 ± 0.0009	11.2913 ± 0.0004
1120	7.9061 ± 0.0006	5.4875 ± 0.0009	11.2948 ± 0.0004
1140	7.8613 ± 0.0007	5.5649 ± 0.0008	11.3132 ± 0.0004

Table S10: Simulation data for OLT deformations of vesicle bilayers with four different sizes, corresponding to the total lipid number $N_{\text{lip}} = 10100$, 6312, 2525, and 1500. The 1st column provides the lipid number N_{ol} within the outer leaflet. The 2nd and 3rd columns display the areas per lipid, a_{il} and a_{ol}, in the inner and outer leaflets as obtained from eqn (S3) using the leaflet radii $R_{\text{le}} = R_{ol}$ and $R_{\text{le}} = R_{il}$ as in eqns (S1) and (S2). The areas per lipid, a_{il} and a_{ol}, in the 4th and 5th column are again obtained from eqn (S3) but with the midsurfaces of the two leaflets computed by eqn (S5). The last two columns display the leaflet tensions Σ_{il} and Σ_{ol} in the inner and outer leaflet as computed using the midsurface radius R_{mid} as determined by the CHAIN protocol.

(a) $N_{\text{lip}} = 10100$

	R_{le} from eqns (S1) and (S2)		R_{le} from eqn (S5)			
N_{ol}	a_{il} $[d^2]$	a_{ol} $[d^2]$	a_{il} $[d^2]$	a_{ol} $[d^2]$	Σ_{il} $[k_{\text{B}}T/d^2]$	Σ_{ol} $[k_{\text{B}}T/d^2]$
5700	1.241 ± 0.008	1.204 ± 0.008	1.095 ± 0.018	1.338 ± 0.019	-0.84 ± 0.07	0.87 ± 0.05
5800	1.263 ± 0.009	1.177 ± 0.009	1.109 ± 0.017	1.303 ± 0.020	-0.54 ± 0.06	0.57 ± 0.04
5900	1.291 ± 0.010	1.155 ± 0.008	1.130 ± 0.018	1.275 ± 0.018	-0.23 ± 0.06	0.26 ± 0.05
5954	1.307 ± 0.014	1.144 ± 0.011	1.147 ± 0.027	1.265 ± 0.024	-0.04 ± 0.06	0.07 ± 0.05
6000	1.322 ± 0.010	1.136 ± 0.009	1.160 ± 0.021	1.257 ± 0.019	0.11 ± 0.05	-0.10 ± 0.06
6100	1.348 ± 0.014	1.112 ± 0.012	1.18 ± 0.03	1.230 ± 0.026	0.40 ± 0.06	-0.40 ± 0.06
6300	1.413 ± 0.020	1.072 ± 0.013	1.23 ± 0.04	1.178 ± 0.025	1.00 ± 0.08	-1.0 ± 0.1

(b) $N_{\text{lip}} = 6312$

	R_{le} from eqns (S1) and (S2)		R_{le} from eqn (S5)			
N_{ol}	a_{il} $[d^2]$	a_{ol} $[d^2]$	a_{il} $[d^2]$	a_{ol} $[d^2]$	Σ_{il} $[k_{\text{B}}T/d^2]$	Σ_{ol} $[k_{\text{B}}T/d^2]$
3641	1.227 ± 0.011	1.204 ± 0.012	1.034 ± 0.023	1.363 ± 0.027	-1.21 ± 0.09	1.21 ± 0.05
3741	1.272 ± 0.015	1.169 ± 0.015	1.069 ± 0.026	1.32 ± 0.03	-0.73 ± 0.07	0.74 ± 0.05
3841	1.321 ± 0.016	1.136 ± 0.013	1.11 ± 0.03	1.281 ± 0.028	-0.23 ± 0.07	0.24 ± 0.06
3858	1.337 ± 0.011	1.138 ± 0.010	1.130 ± 0.024	1.293 ± 0.025	-0.09 ± 0.07	0.11 ± 0.06
3881	1.343 ± 0.015	1.125 ± 0.012	1.127 ± 0.028	1.270 ± 0.025	-0.01 ± 0.07	0.02 ± 0.07
3941	1.380 ± 0.015	1.110 ± 0.011	1.162 ± 0.029	1.255 ± 0.024	0.35 ± 0.08	-0.32 ± 0.08
4041	1.434 ± 0.018	1.078 ± 0.011	1.201 ± 0.029	1.217 ± 0.022	0.83 ± 0.07	-0.84 ± 0.09

(c) $N_{\text{lip}} = 2525$

	R_{le} from eqs. (S1, S2)		$R_{\text{le}} = R_{\text{H}}$			
N_{ol}	a_{il} $[d^2]$	a_{ol} $[d^2]$	a_{il} $[d^2]$	a_{ol} $[d^2]$	Σ_{il} $[k_{\text{B}}T/d^2]$	Σ_{ol} $[k_{\text{B}}T/d^2]$
1575	1.274 ± 0.010	1.216 ± 0.008	0.940 ± 0.021	1.452 ± 0.025	-1.73 ± 0.13	1.73 ± 0.06
1625	1.346 ± 0.009	1.180 ± 0.008	0.984 ± 0.012	1.401 ± 0.015	-1.24 ± 0.10	1.22 ± 0.05
1650	1.380 ± 0.008	1.158 ± 0.007	1.007 ± 0.010	1.374 ± 0.014	-0.92 ± 0.10	0.93 ± 0.05
1675	1.417 ± 0.011	1.139 ± 0.008	1.034 ± 0.014	1.352 ± 0.013	-0.60 ± 0.08	0.61 ± 0.05
1685	1.435 ± 0.007	1.133 ± 0.004	1.048 ± 0.009	1.346 ± 0.008	-0.50 ± 0.08	0.49 ± 0.05
1687	1.434 ± 0.012	1.128 ± 0.008	1.048 ± 0.017	1.340 ± 0.016	-0.45 ± 0.07	0.45 ± 0.06
1695	1.447 ± 0.010	1.122 ± 0.007	1.053 ± 0.014	1.330 ± 0.014	-0.37 ± 0.07	0.34 ± 0.05
1699	1.454 ± 0.011	1.119 ± 0.008	1.062 ± 0.015	1.329 ± 0.014	-0.29 ± 0.10	0.27 ± 0.06
1725	1.506 ± 0.012	1.104 ± 0.007	1.100 ± 0.015	1.311 ± 0.012	0.04 ± 0.06	-0.03 ± 0.05
1775	1.606 ± 0.013	1.071 ± 0.007	1.180 ± 0.017	1.272 ± 0.011	0.76 ± 0.06	-0.74 ± 0.06
1825	1.717 ± 0.021	1.034 ± 0.011	1.264 ± 0.028	1.225 ± 0.019	1.41 ± 0.06	-1.40 ± 0.09

(d) $N_{\text{lip}} = 1500$; data in 1st, 2nd, 5th, and 6th columns plotted in Fig. S5

	R_{le} from eqs. (S1, S2)		$R_{\text{le}} = R_{\text{H}}$			
N_{ol}	a_{il} $[d^2]$	a_{ol} $[d^2]$	a_{il} $[d^2]$	a_{ol} $[d^2]$	Σ_{il} $[k_{\text{B}}T/d^2]$	Σ_{ol} $[k_{\text{B}}T/d^2]$
1030	1.430 ± 0.013	1.183 ± 0.006	0.912 ± 0.017	1.452 ± 0.008	-1.47 ± 0.12	1.49 ± 0.07
1040	1.459 ± 0.013	1.172 ± 0.007	0.928 ± 0.014	1.437 ± 0.009	-1.30 ± 0.15	1.32 ± 0.07
1050	1.490 ± 0.012	1.158 ± 0.008	0.942 ± 0.013	1.415 ± 0.013	-1.12 ± 0.10	1.15 ± 0.07
1060	1.522 ± 0.010	1.146 ± 0.005	0.966 ± 0.009	1.404 ± 0.007	-0.90 ± 0.10	0.94 ± 0.08
1067	1.546 ± 0.012	1.138 ± 0.006	0.983 ± 0.009	1.395 ± 0.010	-0.77 ± 0.13	0.80 ± 0.09
1070	1.557 ± 0.011	1.134 ± 0.006	0.991 ± 0.013	1.390 ± 0.010	-0.71 ± 0.13	0.73 ± 0.07
1080	1.596 ± 0.012	1.124 ± 0.006	1.016 ± 0.007	1.377 ± 0.006	-0.49 ± 0.10	0.51 ± 0.08
1100	1.669 ± 0.015	1.098 ± 0.008	1.068 ± 0.012	1.348 ± 0.009	-0.05 ± 0.11	0.05 ± 0.08
1120	1.749 ± 0.013	1.073 ± 0.005	1.121 ± 0.012	1.318 ± 0.008	0.41 ± 0.12	-0.43 ± 0.07
1140	1.852 ± 0.014	1.050 ± 0.007	1.206 ± 0.016	1.292 ± 0.010	0.94 ± 0.10	-0.9 ± 0.09

Table S11: Radii of nanovesicles with four different sizes and total lipid numbers $N_{\rm lip} = N_{il} + N_{ol} = 10100$, 6312, 2525, and 1500, as obtained *via* the CHAIN protocol. The first column displays the lipid number N_{ol} in the outer leaflet. The lipid number in the inner leaflet is equal to $N_{\rm lip} - N_{ol}$. The different radii are the midsurface radius $R_{\rm mid}$ of the vesicle bilayers; the radii $R_{\rm iH}$ and $R_{\rm oH}$ of the inner and outer leaflet head group layers; and the radii R_{il} and R_{ol}, which represent the midsurfaces of the inner and outer leaflets, used to measure the areas per lipid in these two leaflets.

(a) $N_{\rm lip} = 10100$

N_{ol}	$R_{\rm mid}$ [d]	$R_{\rm iH}$ [d]	$R_{\rm oH}$ [d]	R_{il} [d]	R_{ol} [d]
5700	22.11 ± 0.06	19.58 ± 0.16	24.64 ± 0.18	20.85 ± 0.07	23.37 ± 0.08
5800	22.10 ± 0.05	19.48 ± 0.15	24.53 ± 0.18	20.79 ± 0.07	23.31 ± 0.08
5900	22.11 ± 0.04	19.43 ± 0.16	24.47 ± 0.18	20.77 ± 0.08	23.29 ± 0.09
5954	22.08 ± 0.04	19.45 ± 0.23	24.48 ± 0.24	20.76 ± 0.11	23.28 ± 0.11
6000	22.08 ± 0.04	19.46 ± 0.17	24.50 ± 0.19	20.77 ± 0.08	23.29 ± 0.09
6100	22.04 ± 0.06	19.39 ± 0.24	24.43 ± 0.26	20.72 ± 0.11	23.24 ± 0.12
6300	22.07 ± 0.03	19.27 ± 0.28	24.31 ± 0.26	20.67 ± 0.14	23.19 ± 0.14

(b) $N_{\rm lip} = 6312$

N_{ol}	$R_{\rm mid}$ [d]	$R_{\rm iH}$ [d]	$R_{\rm oH}$ [d]	R_{il} [d]	R_{ol} [d]
3641	17.48 ± 0.06	14.83 ± 0.16	19.87 ± 0.20	16.15 ± 0.07	18.67 ± 0.09
3741	17.48 ± 0.06	14.79 ± 0.18	19.82 ± 0.23	16.13 ± 0.10	18.65 ± 0.12
3841	17.49 ± 0.06	14.75 ± 0.20	19.78 ± 0.21	16.12 ± 0.10	18.64 ± 0.11
3858	17.46 ± 0.05	14.85 ± 0.16	19.92 ± 0.19	16.16 ± 0.07	18.69 ± 0.08
3881	17.47 ± 0.05	14.76 ± 0.18	19.80 ± 0.20	16.12 ± 0.09	18.64 ± 0.10
3941	17.47 ± 0.05	14.81 ± 0.19	19.84 ± 0.19	16.14 ± 0.09	18.65 ± 0.09
4041	17.46 ± 0.05	14.73 ± 0.18	19.78 ± 0.18	16.10 ± 0.10	18.62 ± 0.10

(c) $N_{\rm lip} = 2525$

N_{ol}	$R_{\rm mid}$ [d]	$R_{\rm iH}$ [d]	$R_{\rm oH}$ [d]	R_{il} [d]	R_{ol} [d]
1575	11.20 ± 0.07	8.43 ± 0.10	13.49 ± 0.11	9.81 ± 0.04	12.34 ± 0.04
1625	11.24 ± 0.05	8.39 ± 0.05	13.46 ± 0.07	9.82 ± 0.03	12.35 ± 0.04
1650	11.23 ± 0.05	8.37 ± 0.04	13.43 ± 0.07	9.80 ± 0.03	12.33 ± 0.04
1675	11.21 ± 0.04	8.36 ± 0.06	13.43 ± 0.06	9.79 ± 0.04	12.32 ± 0.04
1685	11.22 ± 0.04	8.37 ± 0.04	13.44 ± 0.04	9.79 ± 0.03	12.33 ± 0.02
1687	11.20 ± 0.04	8.36 ± 0.07	13.41 ± 0.08	9.78 ± 0.04	12.31 ± 0.04
1695	11.21 ± 0.04	8.34 ± 0.06	13.39 ± 0.07	9.78 ± 0.03	12.30 ± 0.04
1699	11.20 ± 0.04	8.36 ± 0.06	13.41 ± 0.07	9.78 ± 0.04	12.30 ± 0.04
1725	11.21 ± 0.04	8.37 ± 0.06	13.41 ± 0.06	9.79 ± 0.04	12.31 ± 0.04
1775	11.19 ± 0.03	8.39 ± 0.06	13.40 ± 0.06	9.79 ± 0.04	12.30 ± 0.04
1825	11.17 ± 0.04	8.39 ± 0.09	13.34 ± 0.10	9.78 ± 0.06	12.25 ± 0.06

(d) $N_{\rm lip} = 1500$

N_{ol}	$R_{\rm mid}$ [d]	$R_{\rm iH}$ [d]	$R_{\rm oH}$ [d]	R_{il} [d]	R_{ol} [d]
1030	8.78 ± 0.05	5.84 ± 0.05	10.91 ± 0.03	7.31 ± 0.03	9.85 ± 0.03
1040	8.79 ± 0.05	5.83 ± 0.04	10.91 ± 0.04	7.31 ± 0.03	9.85 ± 0.03
1050	8.80 ± 0.04	5.81 ± 0.04	10.87 ± 0.05	7.30 ± 0.03	9.84 ± 0.03
1060	8.78 ± 0.04	5.82 ± 0.03	10.88 ± 0.03	7.30 ± 0.02	9.83 ± 0.02
1067	8.78 ± 0.07	5.82 ± 0.03	10.88 ± 0.04	7.30 ± 0.03	9.83 ± 0.03
1070	8.78 ± 0.05	5.82 ± 0.04	10.88 ± 0.04	7.30 ± 0.03	9.83 ± 0.03
1080	8.78 ± 0.05	5.83 ± 0.02	10.88 ± 0.02	7.30 ± 0.03	9.83 ± 0.03
1100	8.75 ± 0.06	5.83 ± 0.03	10.86 ± 0.04	7.29 ± 0.03	9.80 ± 0.03
1120	8.72 ± 0.04	5.82 ± 0.03	10.84 ± 0.03	7.27 ± 0.03	9.78 ± 0.02
1140	8.69 ± 0.04	5.88 ± 0.04	10.83 ± 0.04	7.28 ± 0.03	9.76 ± 0.03

Table S12: Area compressibility moduli and optimal areas per lipid for inner and outer leaflets of nanovesicles with four different total lipid numbers total lipid numbers $N_{\rm lip} = N_{il} + N_{ol}$ as obtained from the VORON protocol *via* eqns (33) and (34) of the main text. The rows display the mean curvatures M_{il} and M_{ol}; the area compressibility moduli K_{il} and K_{ol}; as well as the optimal areas per lipid, a^0_{il} and a^0_{ol} of the inner and outer leaflets, respectively. The optimal areas per lipid and the area compressibility moduli are plotted as green data points in Fig. 11 of the main text.

$N_{\rm lip}$	10100	6312	2525	1500
M_{il} $[1/d]$	-0.049	-0.063	-0.107	-0.147
K_{il} $[k_{\rm B}T/d^2]$	15.5 ± 0.3	15.74 ± 0.20	15.38 ± 0.20	13.89 ± 0.17
a^0_{il} $[d^2]$	1.2755 ± 0.0008	1.2884 ± 0.0006	1.3195 ± 0.0005	1.3422 ± 0.0007
M_{ol} $[1/d]$	0.043	0.053	0.081	0.103
K_{ol} $[k_{\rm B}T/d^2]$	18.0 ± 0.4	20.0 ± 0.5	22.8 ± 0.7	23.8 ± 0.5
a^0_{ol} $[d^2]$	1.1625 ± 0.0008	1.1506 ± 0.0007	1.1291 ± 0.0010	1.1141 ± 0.0007

Table S13: Area compressibility moduli and optimal areas per lipid for inner and outer leaflets of nanovesicles with four different total lipid numbers $N_{\rm lip} = N_{il} + N_{ol}$: (a) Leaflet properties obtained by computing the midsurface radius $R_{\rm mid}$ of the vesicle bilayers *via* the CHAIN protocol, the leaflet radii *via* eqns (S1) and (S2), and the areas per lipid as in eqn (S3). This procedure leads to the blue data points in Fig. 11 and Fig. S6. and (b) Leaflet properties obtained from eqns (S5) and eqn (S3). This procedure leads to the red data points in Fig. S6. The rows of the table display the mean curvatures M_{il} and M_{ol}; the area compressibility moduli K_{il} and K_{ol}; as well as the optimal areas per lipid, a^0_{il} and a^0_{ol} of the inner and outer leaflets, respectively.

(a) Leaflet radii from eqns (S1) and (S2); blue data in Fig. 11 and Fig. S6.

$N_{\rm lip}$	10100	6312	2525	1500
M_{il} $[1/d]$	-0.048	-0.062	-0.102	-0.137
K_{il} $[k_{\rm B}T/d^2]$	15.1 ± 0.3	13.35 ± 0.21	10.80 ± 0.26	9.69 ± 0.09
a^0_{il} $[d^2]$	1.3119 ± 0.0009	1.3464 ± 0.001	1.5051 ± 0.0031	1.6816 ± 0.0016
M_{ol} $[1/d]$	0.043	0.054	0.081	0.102
K_{ol} $[k_{\rm B}T/d^2]$	16.5 ± 0.4	18.6 ± 0.8	21.3 ± 0.4	20.3 ± 0.4
a^0_{ol} $[d^2]$	1.1406 ± 0.0011	1.127 ± 0.0016	1.1067 ± 0.0007	1.0964 ± 0.0008

(b) Leaflet radii from eqn (S5); red data in Fig. S6..

$N_{\rm lip}$	10100	6312	2525	1500
M_{il} $[1/d]$	-0.051	-0.068	-0.119	-0.172
K_{il} $[k_{\rm B}T/d^2]$	15.4 ± 0.5	13.6 ± 0.5	10.5 ± 0.3	9.20 ± 0.05
a^0_{il} $[d^2]$	1.1517 ± 0.0015	1.1316 ± 0.0019	1.097 ± 0.0019	1.0729 ± 0.0004
M_{ol} $[1/d]$	0.041	0.05	0.075	0.092
K_{ol} $[k_{\rm B}T/d^2]$	15.2 ± 0.6	18 ± 1	21.4 ± 0.8	21.95 ± 0.22
a^0_{ol} $[d^2]$	1.2609 ± 0.002	1.2738 ± 0.0032	1.3138 ± 0.0013	1.3455 ± 0.0004

Table S14: Elastic deformations by vesicle inflation and deflation (VID) for a nanovesicle with $N_{il} = 840$ lipids in the inner leaflet and $N_{ol} = 1685$ lipids in the outer one, corresponding to the reference state with tensionless leaflets for total lipid number $N_{\rm lip} = N_{il} + N_{ol} = 2525$. The rows display the number of water beads inside and outside of the vesicle, $N_{i\rm W}$ and $N_{o\rm W}$; the volume $V_{i\rm W}$ of the interior water compartment; as well as the leaflet tensions Σ_{il} and Σ_{ol} of the inner and outer leaflets, as computed *via* the VORON protocol, see green data in Fig. 12.

$N_{i\rm W}$	$N_{o\rm W}$	$V_{i\rm W}$	Σ_{il} $[k_{\rm B}T/d^2]$	Σ_{ol} $[k_{\rm B}T/d^2]$
10000	158340	3306.7 ± 0.7	2.71 ± 0.05	1.36 ± 0.04
9000	159340	2985.5 ± 0.6	2.11 ± 0.04	0.92 ± 0.04
8000	160340	2663.7 ± 0.5	1.40 ± 0.04	0.51 ± 0.03
7000	161340	2341.2 ± 0.5	0.56 ± 0.07	0.15 ± 0.05
6900	161440	2309.1 ± 0.7	0.50 ± 0.05	0.12 ± 0.04
6800	161630	2276.5 ± 0.6	0.39 ± 0.06	0.11 ± 0.05
6700	161640	2244.2 ± 0.5	0.29 ± 0.06	0.08 ± 0.05
6500	161840	2179.3 ± 0.6	0.12 ± 0.06	0.03 ± 0.06
6200	162230	2081.4 ± 0.5	-0.16 ± 0.08	0.04 ± 0.07
6100	162330	2048.6 ± 0.6	-0.32 ± 0.07	0.13 ± 0.10
6050	162380	2032.1 ± 0.6	-0.33 ± 0.06	0.09 ± 0.08
6000	162430	2015.7 ± 0.8	-0.36 ± 0.06	0.13 ± 0.10

Table S15: To study the OLT deformations of nanovesicles, these vesicles were initially assembled with a total number of $N_{\rm lip}$ lipids, chosing the initial radius $R_{\rm ini}$ and the fixed number $N_{o\rm W}$ of water beads outside the vesicle to fill up the cubic simulation box with linear dimension L. We then varied the lipid numbers N_{il} and N_{ol} for fixed $N_{\rm lip} = N_{ol} + N_{il}$ and adjusted the number $N_{i\rm W}$ of water beads inside the vesicle to obtain a tensionless bilayer. The adjusted water bead numbers $N_{i\rm W}$ are displayed in the third rows of the subtables.

(a) $N_{\rm lip} = 10100$, $R_{\rm ini} = 22.1\,d$, $N_{o\rm W} = 1350000$, and $L = 80\,d$

N_{il}	N_{ol}	$N_{\rm iW}$
3800	6300	88400
4000	6100	87400
4100	6000	87400
4146	5954	87400
4200	5900	87420
4300	5800	87300
4400	5700	87350

(b) $N_{\rm lip} = 6312$, $R_{\rm ini} = 17.5\,d$ $N_{o\rm W} = 437845$, and $L = 55\,d$

N_{il}	N_{ol}	$N_{\rm iW}$
2271	4041	38250
2371	3941	38000
2431	3881	37800
2454	3858	37770
2471	3841	37750
2571	3741	37600
2671	3641	37480

(c) $N_{\rm lip} = 2525$, $R_{\rm ini} = 11.2\,d$ $N_{o\rm W} = 162000$, and $L = 40\,d$

N_{il}	N_{ol}	$N_{\rm iW}$
950	1575	6050
900	1625	6250
875	1650	6290
850	1675	6330
840	1685	6430
838	1687	6340
830	1695	6350
826	1699	6350
800	1725	6430
750	1775	6580
700	1825	6790

(d) $N_{\rm lip} = 1500$, $R_{\rm ini} = 8\,d$ $N_{\rm ow} = 90000$, and $L = 32\,d$

N_{il}	N_{ol}	$N_{\rm iW}$
360	1140	2150
380	1120	2060
400	1100	2035
420	1080	2000
430	1070	1980
433	1067	1974
440	1060	1960
450	1050	1940
460	1040	1920
470	1030	1900